Supplementary Materials

Supplementary Figure Legends

Figure S1. Structure-based sequence alignments of ScPif1p, BsPif1 and human Pif1. The secondary structure elements of ScPif1p are shown above the sequence, as cylinders (for α- and η-helices) and arrows (for β-strands). The domain sequences are colored according to the color scheme in Figure 1A and labeled sequentially within each domain. The highly conserved residues are boxed. Only amino acid sequences corresponding to the nuclear-form ScPif1p (aa 40–859) are shown for comparison.

Figure S2. Purifications and characterizations of ScPif1p. (**A**) Coomassie Blue-stained 10% SDS-polyacrylamide gel of purified truncated (aa 237–780) ScPif1p loaded with 20 (lane 1), 4 (lane 2), and 1 μg (lane 3). The molecular-mass standards (lane 4) (in kDa) are shown on the right. (**B**) Unwinding kinetics of the full-length nuclear form (aa 40–859) and the truncated (aa 237–780) ScPif1p proteins. The assays were performed with 4 nM fluorescently labeled partial duplex DNA ($S_{26}ds_{17}$) and 100 nM proteins as described under "Materials and Methods". The plots shown are representative of three independent experiments. (**C**) Size exclusion chromatography analysis of ScPif1p by Superdex 200 10/300 GL. The protein molecular standards are indicated above the elution curve. The apparent molecular weight of ScPif1p is 63 kDa, in accordance with a monomeric protein. **(D–F**) Radius distributions of ScPif1p (D), ScPif1p in complex with ssDNA (Poly(T_{11})) (E) and with partial dsDNA (8T11bp) (F), obtained from analyses of experimental data in DLS assays. The experiments were carried out as described under "Materials and Methods". The determined hydrodynamic radii are between 3.98–4.11 nm, corresponding to a monomeric ScPif1p with *M*w of ~63 kDa.

Figure S3. Crystal packing of ScPif1p and identification of the dimers. (**A**) Crystal of ScPif1p in P212121 space group contains two molecules in the asymmetric unit. The two distinct molecules are colored in cyan (molecule A) and green (molecule B) in the whole unit cell of the crystal. (**B**) In the same P212121 unit cell, the non-crystallographic relationships between the molecules are highlighted. The translational non-crystallographic symmetry is shown between molecule B in light blue and molecule A in cyan. Several dimers can be isolated in the unit cell: dimer 1 (pair cyan/green), dimer 2 (pair cyan/blue), dimer 3 (pair cyan/pink) and dimer 4 pair (cyan/yellow). (**C**) P3121 crystals contain two ScPif1p molecules (colored green and cyan) in the asymmetric

unit. The two molecules in cyan are related by a two-fold crystallographic symmetry and correspond to the dimer 2 in the P212121 unit cell.

Figure S4. Comparison of nucleotide binding sites in human Pif1 and ScPif1p. (**A**) Structure of the nucleotide binding site in human Pif1 (PDB entry 5FHH). The structure was refined to R/R_{free} = 32.9/36.9. The electron density calculated from the deposited Structure Factors is contoured at 1.2. The orientation is the same as that is Figure 1E. (**B**) After refinement of human Pif1 with R/R_{free} =27.5/34.1, the spatial position of ADP·AlF_4 ligand undergoes a significant change which is equivalent to the position of ADP·AlF_4 ligand in ScPif1p. The resulting electron density map is contoured at 1.2. (**C**) Overlay of nucleotide binding sites of human Pif1 and ScPif1p. Human Pif1 and ScPif1p Cα backbones superimpose with r.m.s.d of 2.0 Å. 5FHH is shown in pink, refined human Pif1 in cyan and ScPif1p in green. The ligand ADP·AlF_4 is shown as sticks and the magnesium ion as a sphere. (**D**) Stopped-flow DNA unwinding curves for ScPif1p variant Q241A with different NTPs, which are used to determine the DNA unwinding amplitude and rate of the variant. The assays were performed with 200 nM mutant Q241A, 4 nM fluorescently labeled partial duplex DNA under experimental conditions as described in "Materials and Methods"**.**

Figure S5. (**A**) Superimposition of domain 2C of ScPif1p (aa 542–651) in yellow on RecB (aa 607–647) in pink. (**B**) Details of the cryoEM structure of RecBCD (PDB entry 5LD2), only RecB and RecD are shown. (**C**) ScPif1p is in the same orientation as RecD in (B). Domain 1A of RecD and that of ScPif1p have been superimposed in order to have the best fit for ssDNA complexed in both molecules. (**D**) Superimposition of ScPif1p on the RecBCD structure. Domain 2C of ScPif1p superimposes on RecB (the analogous structural domain is shown in pink).

Figure S6. SEC-SAXS profiles of all data collected, processed with HPLC-SAXS module of US-SOMO. During elution, SAXS data $I(q)$ are collected during time t. $I(q, t)$ are transformed as $I(t, q)$. The 'experimental' SAXS curve $I(t, q)$ recorded at the lowest q value (0.006) is shown. Deconvoluted peaks from Gaussian approximations are indicated in different colors and the calculated Radius of gyrations are plotted. In the lower panels the absorbances at 260 and 280 nm are indicated on the same time scale. Profiles for 3G4 and 8T3G4 are shown in (**A**) and (**B**), respectively. Profiles for apo ScPif1p, ScPif1p in complex with ssDNA (GR_{11}) in the presence of ADP·AlF_4, or with 8T3G4, 3G4 and 8T11bp, are shown in C, D, E, F and G, respectively.

Figure S7. Normalized Krakty plots and pair distance distribution functions showing comparison of apo ScPif1p and ScPif1p-ssDNA (GR_{11}) complex (**A** and **B**), and of G-quadruplexes 3G4 and 8T3G4 (**C** and **D**).

Figure S8. Ensemble Optimization Method (EOM) calculation for 10000 models of apo ScPif1p and ScPif1p-ssDNA (GR_{11}) complex. Flexibility has been introduced between the 2B + 2C domain and the rest of the protein. Distribution of *R*g and *D*max for the pool (red) and ensemble (green) are given for apo ScPif1p (**A** and **B**) and for the complex (**C** and **D**). For the apo protein, the distributions show an ensemble with at least two populations which are reduced to a single population for the complex.

Figure S9. Summary of calculated fits of models to SAXS experimental data. For clarity, the models are shown in surface representations with colors according to the color scheme in Figure 1. The DNAs are shown in green, light green and dark green bound to each monomer in the dimers model. The residuals are calculated as experimental intensity divided by computed intensity. The models tested and the corresponding fits are shown for apo-ScPif1p (A), ScPif1p-ssDNA (GR_{11}) complex (B), 3G4 (C), 8T3G4 (D), ScPif1p-8T3G4 complex (E), Dimer1-8T3G4 complex (F), Dimer2-8T3G4 complex (G), Dimer3-8T3G4 complex (H), Dimer4-8T3G4 complex (I), Dimer2-3G4 complex (J), ScPif1p-8T11bp complex (K) and Dimer2-8T11bp complex (L). For dimers, several stoeichiometry hypothesis have been tested and are indicated as protein:DNA ratio after the dimer name. The comparisons of experimental and model data are presented in Table S4.

Figure S10. (**A**) Anisotropy-based DNA binding isotherms of ScPif1p with ssDNA Poly(T_{12}), dsDNA ($dsDNA_{16bp}$), and F-$G4_{17}$. The binding curve of variant DM F-$G4_{17}$ is also determined under the same experimental conditions. The insert is an enlarged show of cooperative and non cooperative binding curve for wild-type ScPif1p and DM, respectively. The solid lines represent the best fits of the data with Equation 1 for ss- and dsDNA, or with the Hill equation for ScPif1p in complex with F-$G4_{17}$ (H_n = 2.08 ± 0.1). (**B**) Gel filtration analysis of apo ScPif1p (green line) and ScPif1p in complex with ssDNA Poly(T_{22}) (blue line) and 8T3G4 (red line), respectively. DM mutant in complex with 8T3G4 (black line) was also analyzed under the same experimental conditions. The elution profiles were recorded from a Superdex 200 column (GE Healthcare) at a protein concentration of 10 mg/ml. Molecular weights used for the calibration are indicated on the top axis.

Figure S1

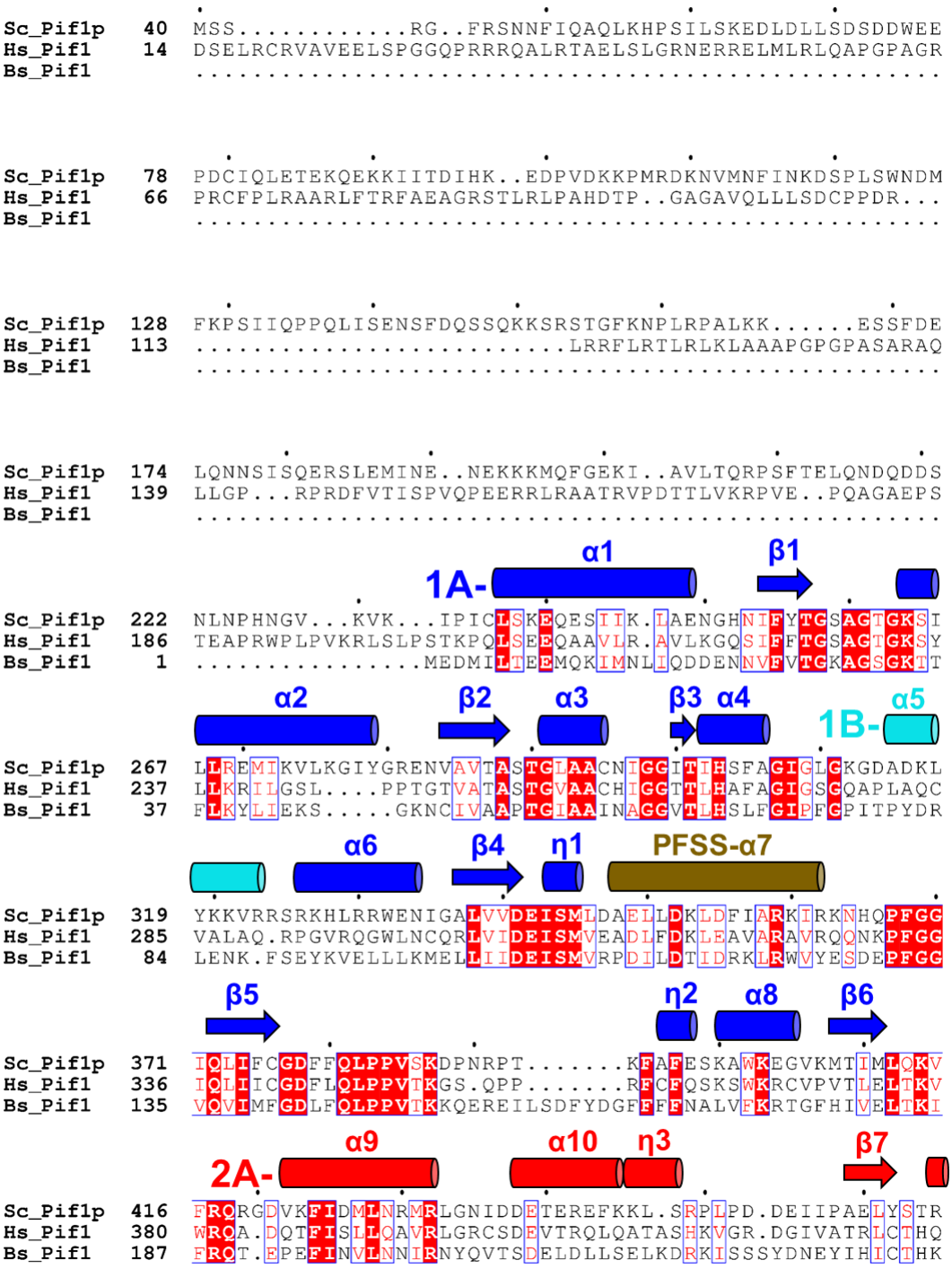
Sc_Pif1p 40 MSS.....RG..FRSNNFIQAQLKHPSILSKEDLDLLSDSDDWEE
Hs_Pif1 14 DSELRCRVAVEELSPGGQPRRRQALRTAELSLGRNERRELMLRLQAPGPAGR
Bs_Pif1 .....
Sc_Pif1p 78 PDCIQLETEKQEKKIITDIHK..EDPVDKKPMRDKNVMNFINKDSPLSWNDM
Hs_Pif1 66 PRCFPLRAARLFTRFAEAGRSTLRLPAHDTP..GAGAVQLLLSDCPPDR...
Bs_Pif1 .....
Sc_Pif1p 128 FKPSIIQPPQLISENSFDQSSQKKSRSTGFKNPLRPALKK......ESSFDE
Hs_Pif1 113 .....LRRFLRTLRLKLAAAPGPGPASARAQ
Bs_Pif1 .....
Sc_Pif1p 174 LQNNSISQERSLEMINE..NEKKKMQFGEKI..AVLTQRPSFTELQNDQDDS
Hs_Pif1 139 LLGP...RPRDFVTISPVQPEERRLRAATRVPDTTLVKRPVE..PQAGAEPS
Bs_Pif1 .....
α1
β1
1A-
Sc_Pif1p 222 NLNPHNGV...KVK...IPICLSKEQESIIK.LAENGHNIFYTGSAGTGKSI
Hs_Pif1 186 TEAPRWPLPVKRLSLPSTKPQLSEEQAAVLR.AVLKGQSIFFTGSAGTGKSY
Bs_Pif1 1 .....MEDMILTEEMQKIMNLIQDDENNVFVTGKAGSGKTT
α2
β2
α3
β3
α4
α5
1B-
Sc_Pif1p 267 LLREMIKVLKGIYGRENVAVTASTGLAACNIGGITIHSFAGIGLGKGDADKL
Hs_Pif1 237 LLKRILGSL....PPTGTVATASTGVAACHIGGTTLHAFAGIGSGQAPLAQC
Bs_Pif1 37 FLKYLIEKS.....GKNCIVAAPTGIAAINAGGVTLHSLFGIPFGPITPYDR
α6
β4
η1
PFSS-α7
Sc_Pif1p 319 YKKVRRSRKHLRRWENIGALVVDEISMLDAELLDKLDFIARKIRKNHQPFGG
Hs_Pif1 285 VALAQ.RPGVRQGWLNCQRLVIDEISMVEADLFDKLEAVARAVRQQNKPFGG
Bs_Pif1 84 LENK.FSEYKVELLLKMELLIIDEISMVRPDILDTIDRKLRWVYESDEPFGG
β5
η2
α8
β6
Sc_Pif1p 371 IQLIFCGDFFQLPPVSKDPNRPT.....KFAFESKAWKEGVKMTIMLQKV
Hs_Pif1 336 IQLIICGDFLQLPPVTKGS.QPP.....RFCFQSKSWKRCVPVTLELTKV
Bs_Pif1 135 VQVIMFGDLFQLPPVTKKQEREILSDFYDGFFFFNALVFKRTGFHIVELTKI
α9
α10
η3
β7
2A-
Sc_Pif1p 416 FRQRGDVKFIDMLNRMRLGNIDDETEREFKKL.SRPLPD.DEIIPAELYSTR
Hs_Pif1 380 WRQA.DQTFISLLQAVRLGRCSDEVTRQLQATASHKVGR.DGIVATRLCTHQ
Bs_Pif1 187 FRQT.EPEFINVLNNIRNYQVTSDELDLLSELKDRKISSSYDNEYIHICTHK

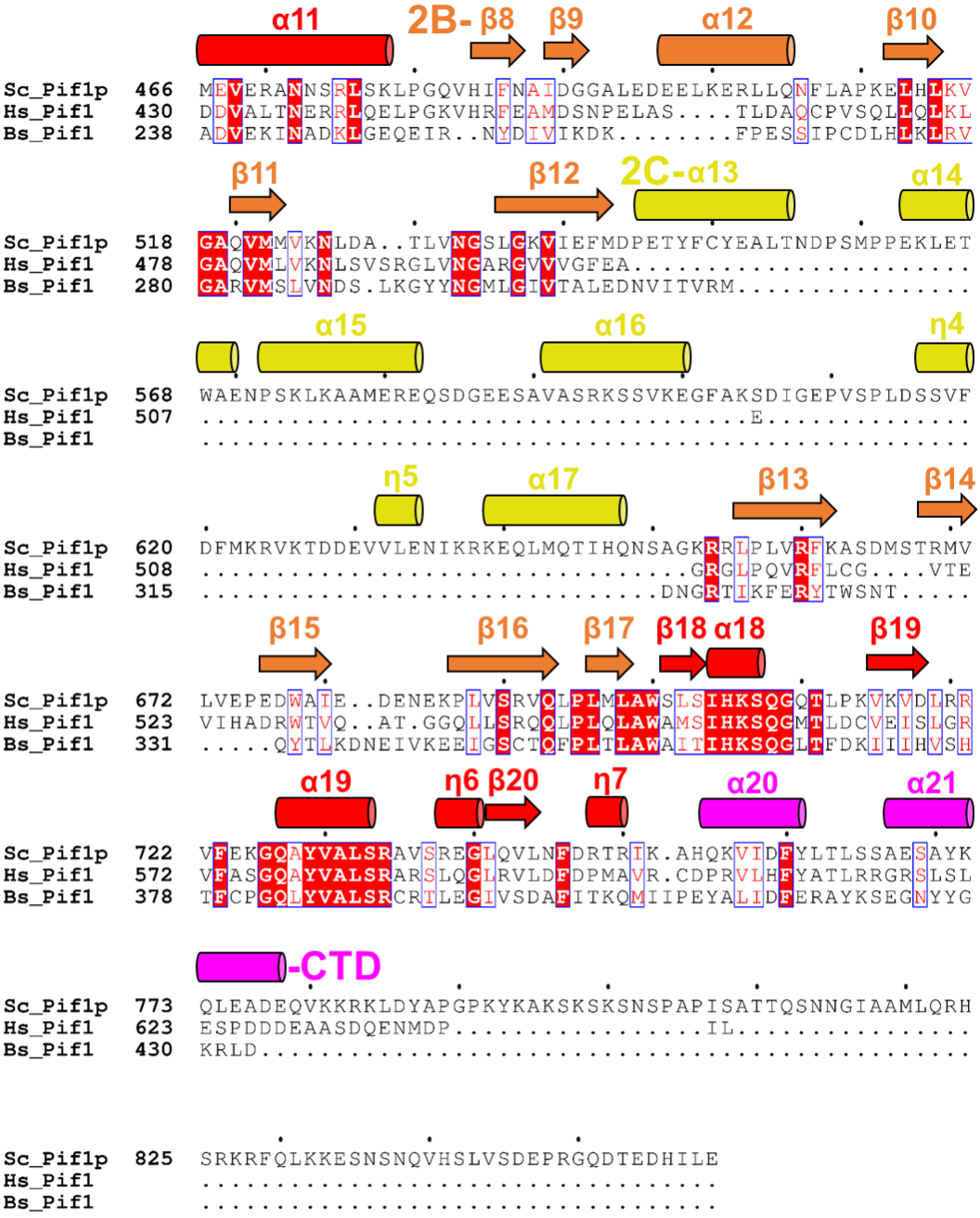
α11
2B-
β8
β9
α12
β10
Sc_Pif1p 466 MEVERANNSRLSKLPGQVHIFNAIDGGALEDEELKERLLQNFLAPKELHLKV
Hs_Pif1 430 DDVALTNERRLQELPGKVHRFEAMDSNPELAS....TLDAQCPVSQLLQLKL
Bs_Pif1 238 ADVEKINADKLGEQEIR..NYDIVIKDK.....FPESSIPCDLHLKLRV
β11
β12
2C-α13
α14
Sc_Pif1p 518 GAQVMMVKNLDA..TLVNGSLGKVIEFMDPETYFCYEALTNDPSMPPEKLET
Hs_Pif1 478 GAQVMLVKNLSVSRGLVNGARGVVVGFEA.....
Bs_Pif1 280 GARVMSIVNDS.LKGYYNGMLGIVTALEDNVITVRM.....
α15
α16
η4
Sc_Pif1p 568 WAENPSKLKAAMEREQSDGEESAVASRKSSVKEGFAKSDIGEPVSPLDSSVF
Hs_Pif1 507 .....E.....
Bs_Pif1 .....
η5
α17
β13
β14
Sc_Pif1p 620 DFMKRVKTDDEVVLENIKRKEQLMQTIHQNSAGKRRLPLVRFKASDMSTRMV
Hs_Pif1 508 .....GRGLPQVRFLCG....VTE
Bs_Pif1 315 .....DNGRTIKFERYTWSNT.....
β15
β16
β17
β18
α18
β19
Sc_Pif1p 672 LVEPEDWAIE..DENEKPLVSRVQLPLMLAWSLSIHKSQGQTLPKVKVDLRR
Hs_Pif1 523 VIHADRWTVQ..AT.GGQLLSRQQLPLQLAWAMSIHKSQGMTLDCVEISLGR
Bs_Pif1 331 .....QYTLKDNEIVKEEIGSCTQFPLTLAWAITIHKSQGLTFDKIIIHVSH
α19
η6
β20
η7
α20
α21
Sc_Pif1p 722 VFEKGQAYVALSRAVSREGLQVLNFDRTRIK.AHQKVIDFYLTLSSAESAYK
Hs_Pif1 572 VFASGQAYVALSRARSLQGLRVLDFDPMAVR.CDPRVLHFYATLRRGRSLSL
Bs_Pif1 378 TFCPGQLYVALSRCRTLEGIVSDAFITKQMIIPEYALIDFERAYKSEGNYYG
-CTD
Sc_Pif1p 773 QLEADEQVKKRKLDYAPGPKYKAKSKSKSNSPAPISATTQSNNGIAAMLQRH
Hs_Pif1 623 ESPDDDEAASDQENMDP.....IL.....
Bs_Pif1 430 KRLD.....
Sc_Pif1p 825 SRKRFQLKKESNSNQVHSLVSDEPRGQDTEDHILE
Hs_Pif1 .....
Bs_Pif1 .....

Figure S2

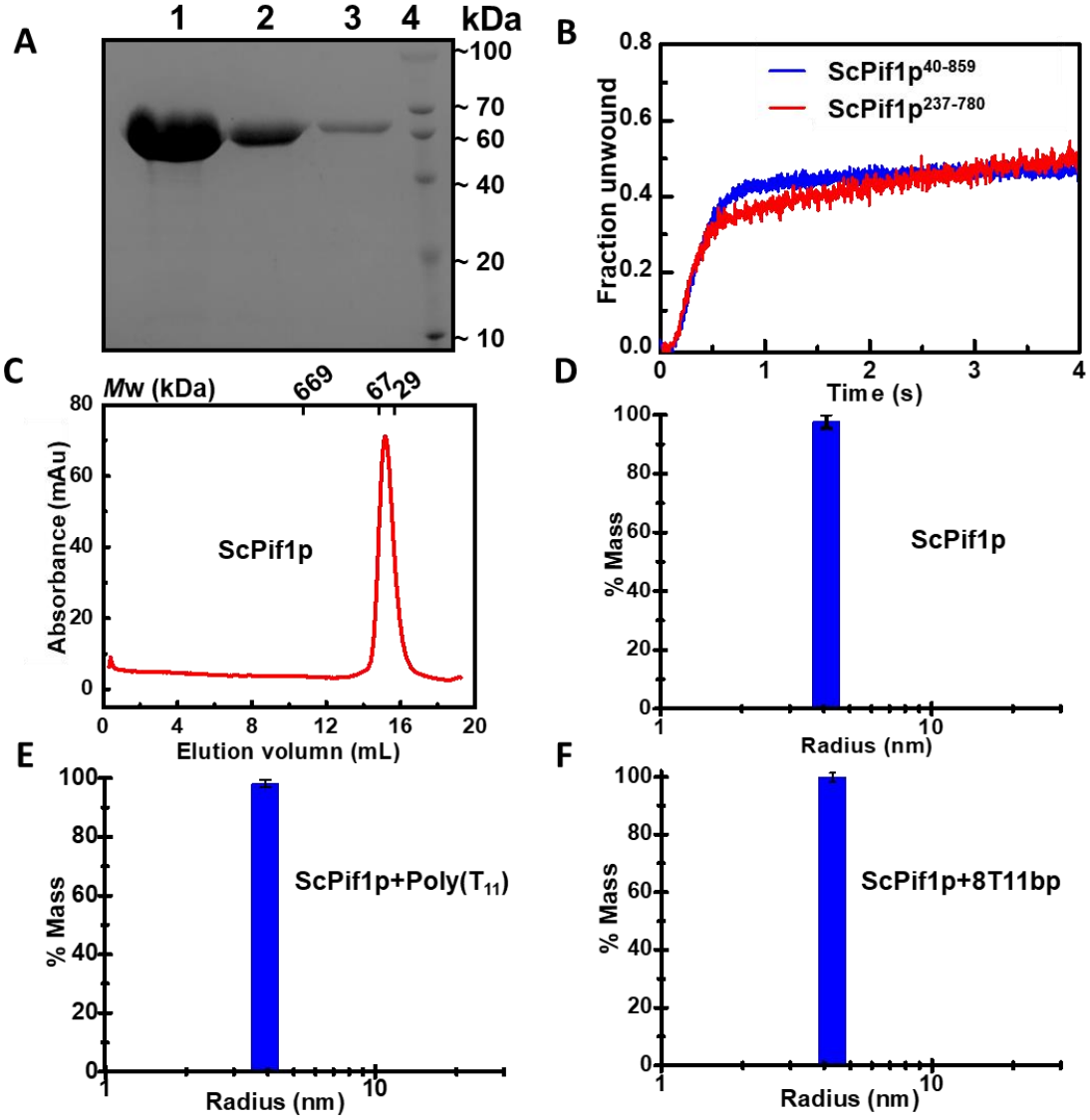
A
1
2
3
4
kDa
100
70
60
40
20
10
B
ScPif1p40-859
ScPif1p237-780
Fraction unwound
Time (s)
C
Mw (kDa)
669
67
29
ScPif1p
Absorbance (mAu)
Elution volumn (mL)
D
ScPif1p
% Mass
Radius (nm)
E
ScPif1p+Poly(T11)
% Mass
Radius (nm)
F
ScPif1p+8T11bp
% Mass
Radius (nm)

Figure S3

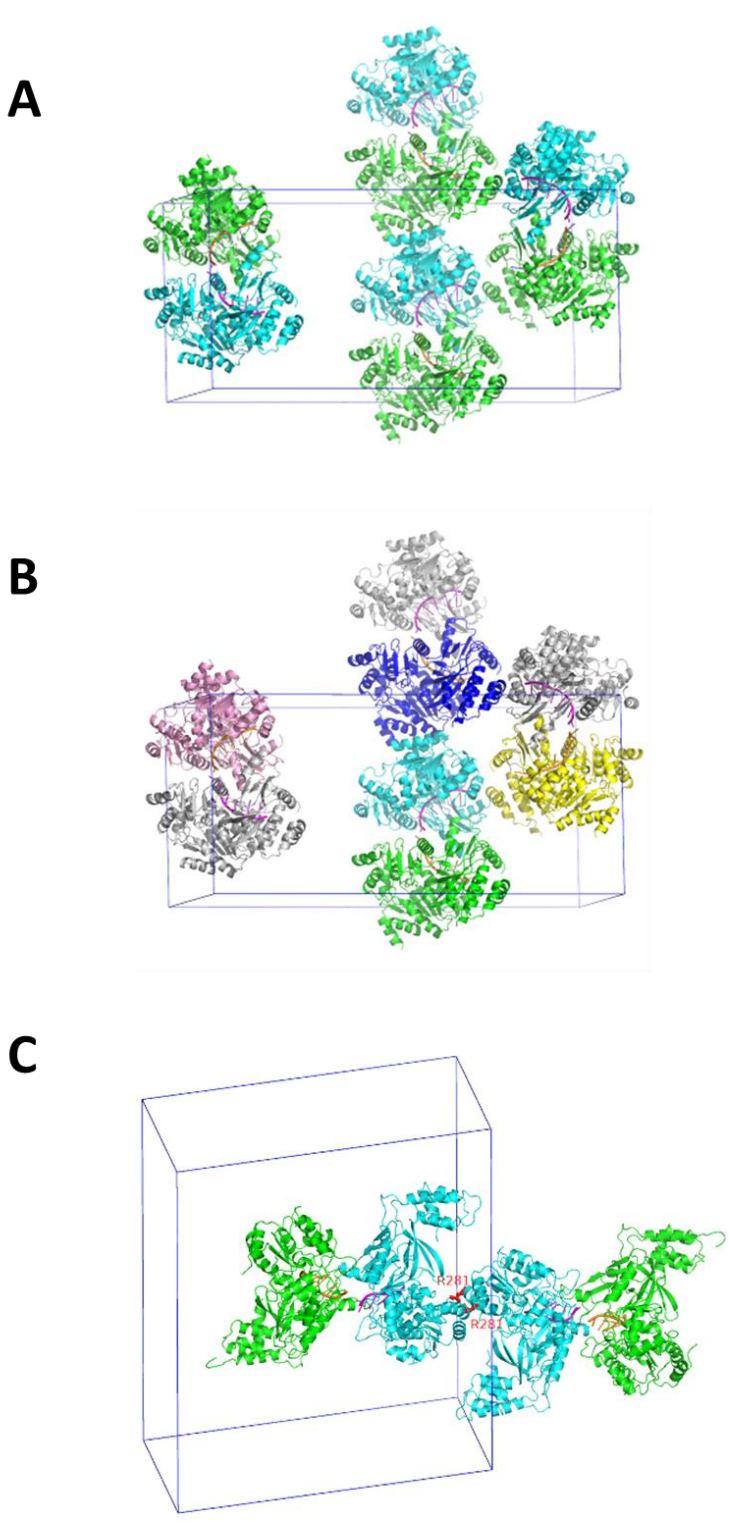

Figure S4

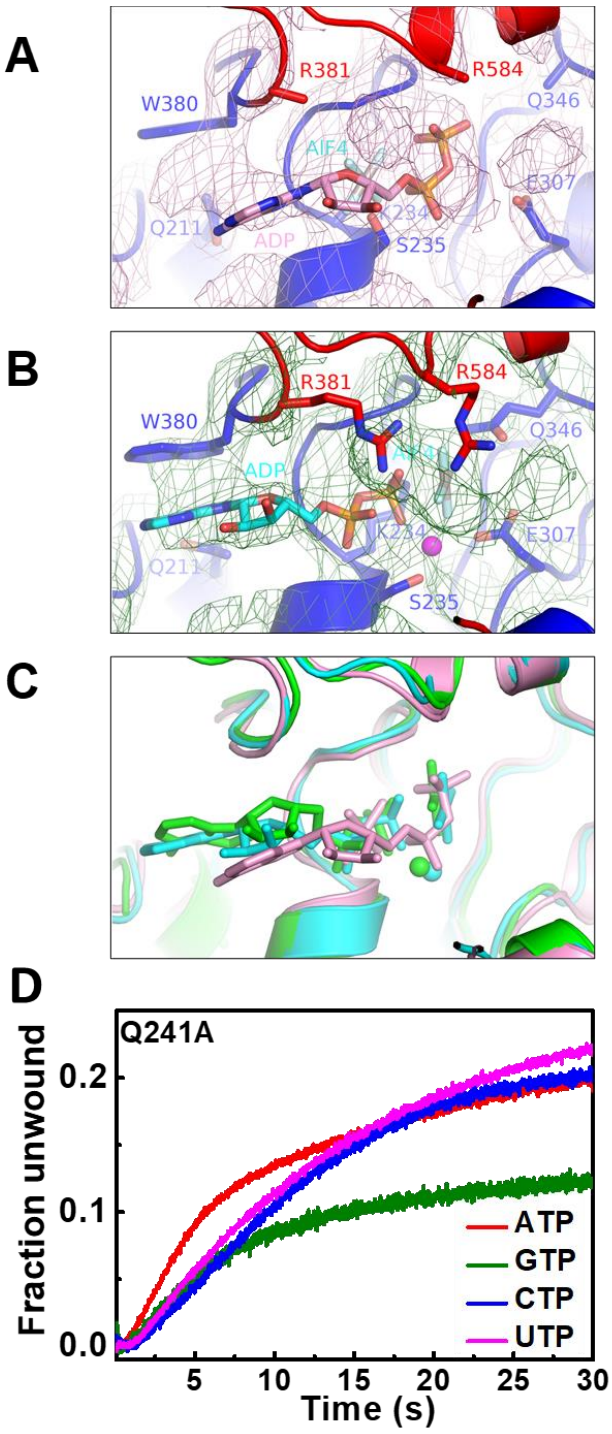
A
R381
R584
W380
Q346
AlF4
E307
Q211
K234
ADP
S235
B
R381
R584
W380
Q346
ADP
K234
E307
Q211
S235
C
D
Q241A
Fraction unwound
0.0
0.1
0.2
5
10
15
20
25
30
Time (s)
ATP
GTP
CTP
UTP

Figure S5

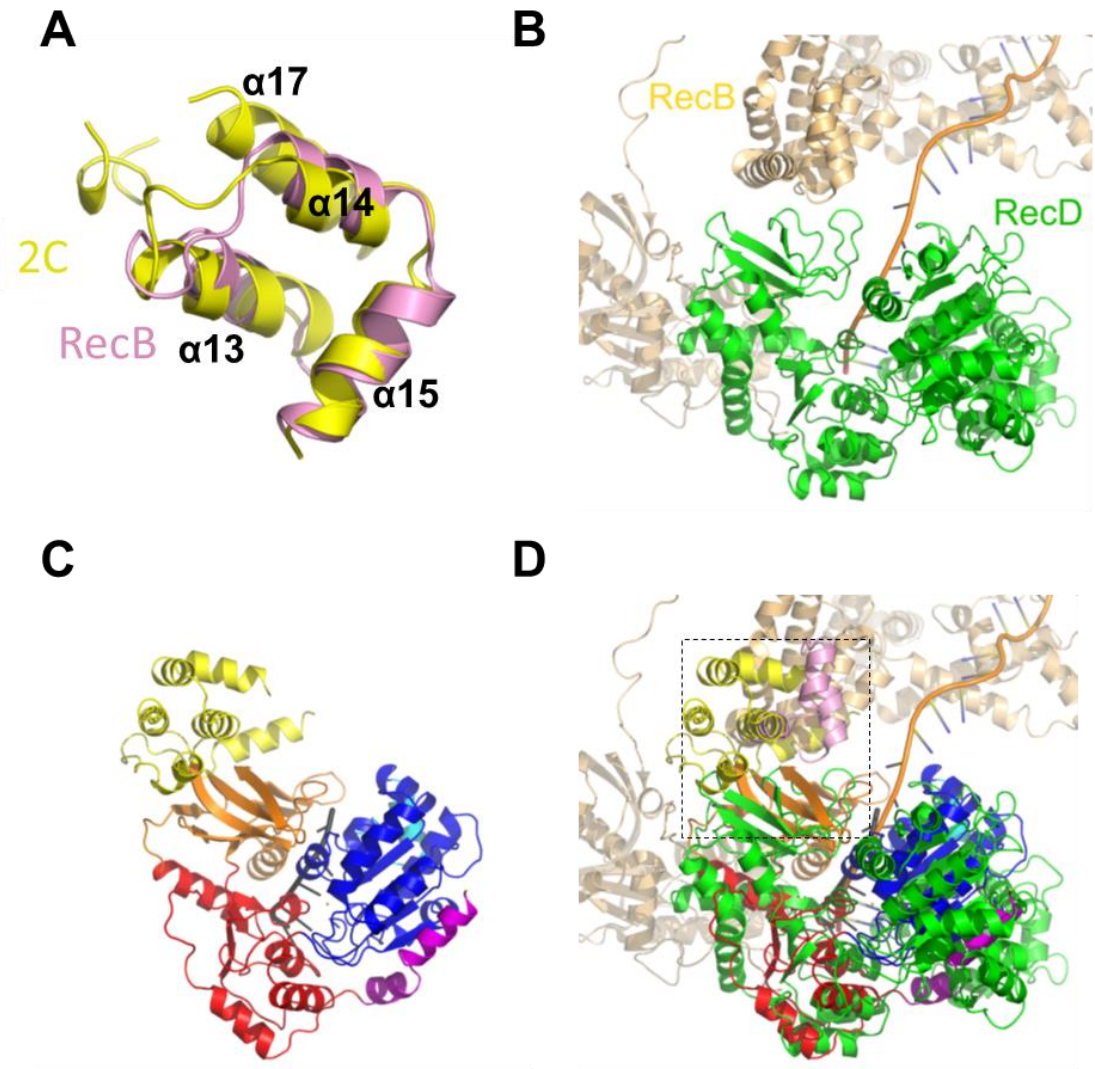

Figure S6

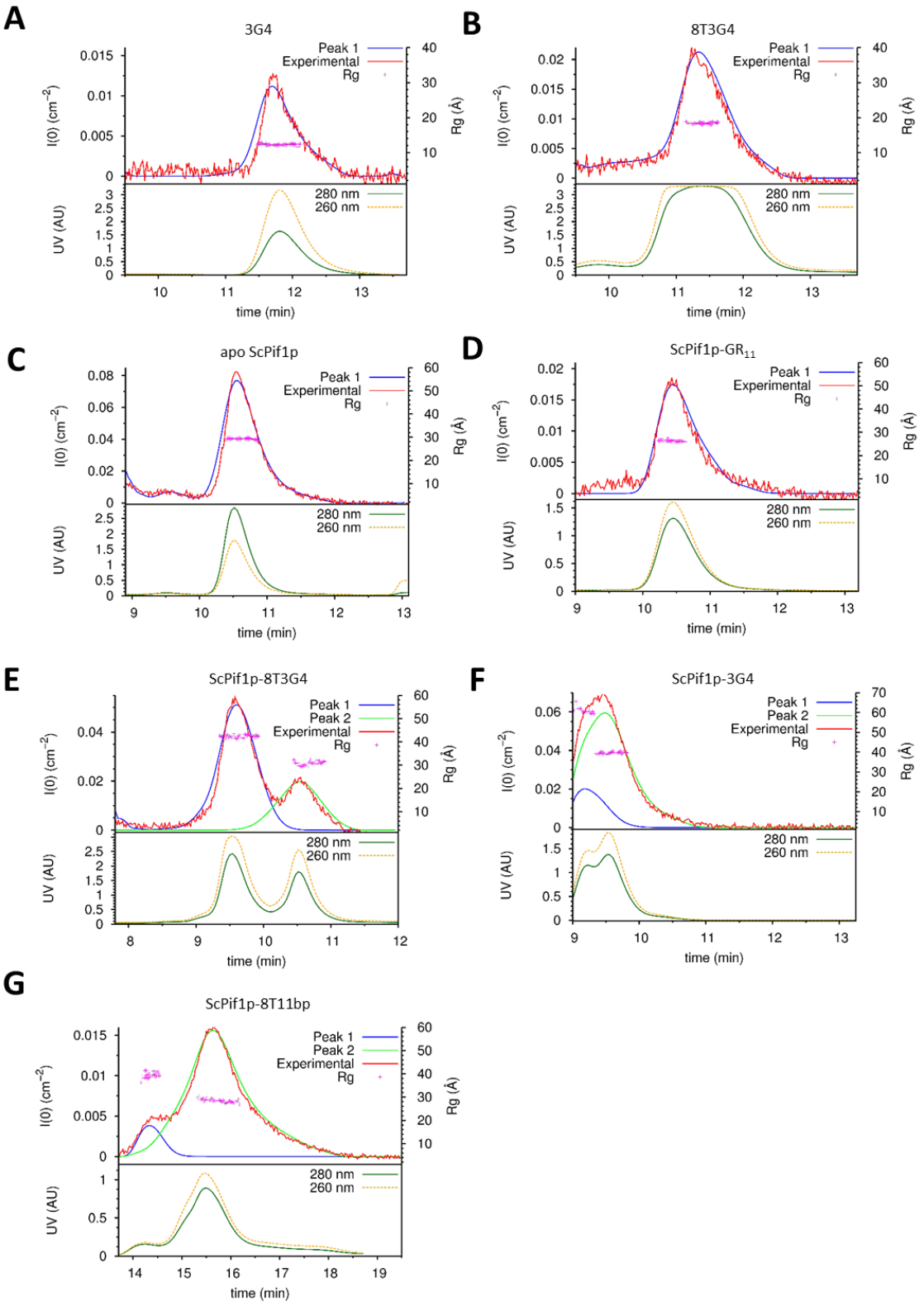
A
3G4
B
8T3G4
C
apo ScPif1p
D
ScPif1p-GR11
E
ScPif1p-8T3G4
F
ScPif1p-3G4
G
ScPif1p-8T11bp
Peak 1
Peak 2
Experimental
Rg
280 nm
260 nm
I(0) (cm−2)
Rg (Å)
UV (AU)
time (min)

Figure S7

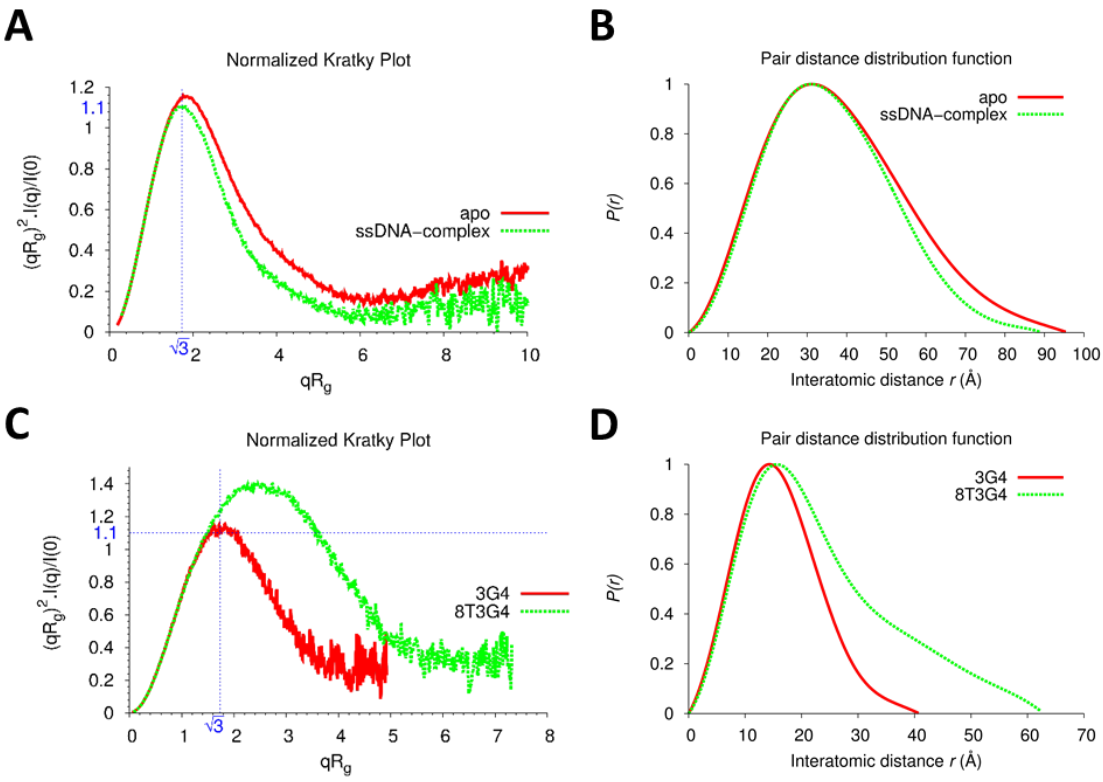
A
Normalized Kratky Plot
$(qR_g)^2.I(q)/I(0)$
qR_g
apo
ssDNA–complex
B
Pair distance distribution function
P(r)
Interatomic distance r (Å)
apo
ssDNA–complex
C
Normalized Kratky Plot
$(qR_g)^2.I(q)/I(0)$
qR_g
3G4
8T3G4
D
Pair distance distribution function
P(r)
Interatomic distance r (Å)
3G4
8T3G4

Figure S8

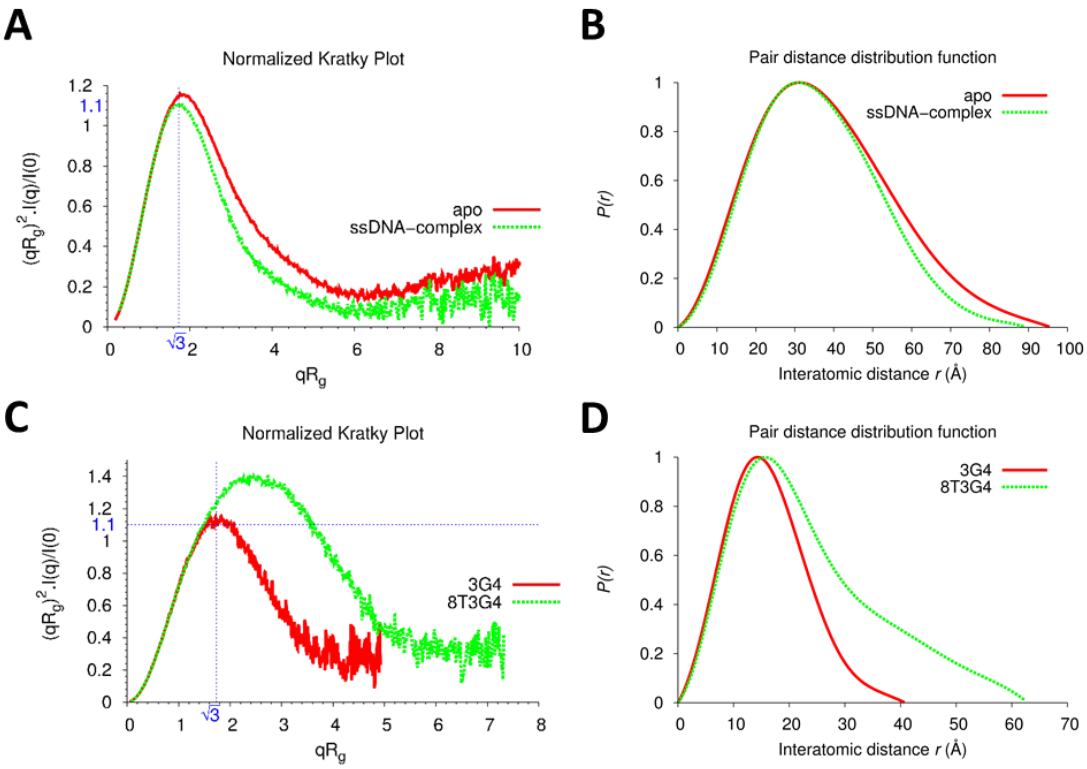
A
Normalized Kratky Plot
$(qR_g)^2.I(q)/I(0)$
qR_g
√3
apo
ssDNA–complex
B
Pair distance distribution function
P(r)
Interatomic distance r (Å)
apo
ssDNA–complex
C
Normalized Kratky Plot
$(qR_g)^2.I(q)/I(0)$
qR_g
√3
3G4
8T3G4
D
Pair distance distribution function
P(r)
Interatomic distance r (Å)
3G4
8T3G4

Figure S9

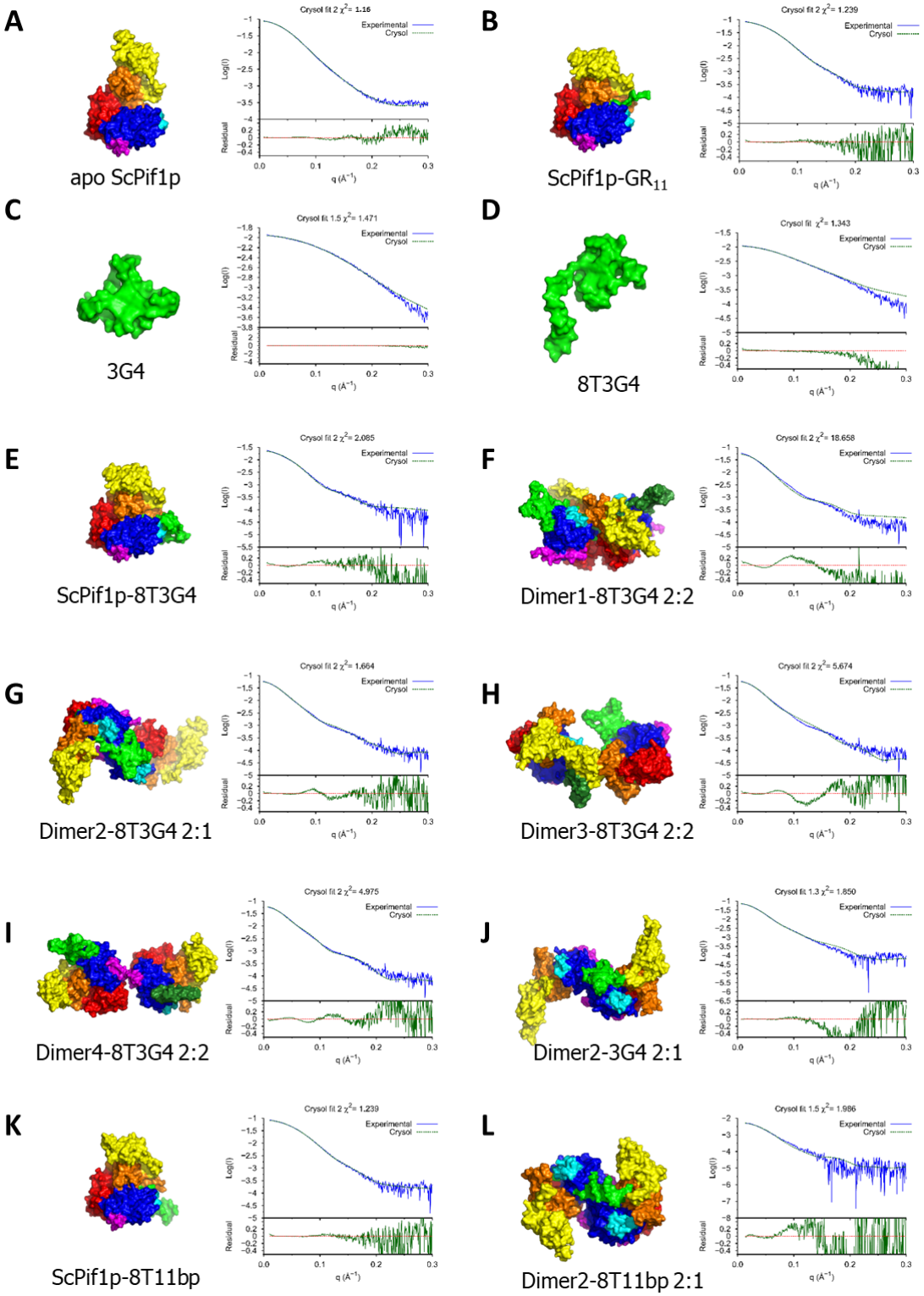
A
apo ScPif1p
Crysol fit 2 χ²= 1.16
B
ScPif1p-GR11
Crysol fit 2 χ²= 1.239
C
3G4
Crysol fit 1.5 χ²= 1.471
D
8T3G4
Crysol fit χ²= 1.343
E
ScPif1p-8T3G4
Crysol fit 2 χ²= 2.085
F
Dimer1-8T3G4 2:2
Crysol fit 2 χ²= 18.658
G
Dimer2-8T3G4 2:1
Crysol fit 2 χ²= 1.664
H
Dimer3-8T3G4 2:2
Crysol fit 2 χ²= 5.674
I
Dimer4-8T3G4 2:2
Crysol fit 2 χ²= 4.975
J
Dimer2-3G4 2:1
Crysol fit 1.3 χ²= 1.850
K
ScPif1p-8T11bp
Crysol fit 2 χ²= 1.239
L
Dimer2-8T11bp 2:1
Crysol fit 1.5 χ²= 1.986
Experimental
Crysol
Log(I)
Residual
q (Å⁻¹)

Figure S10

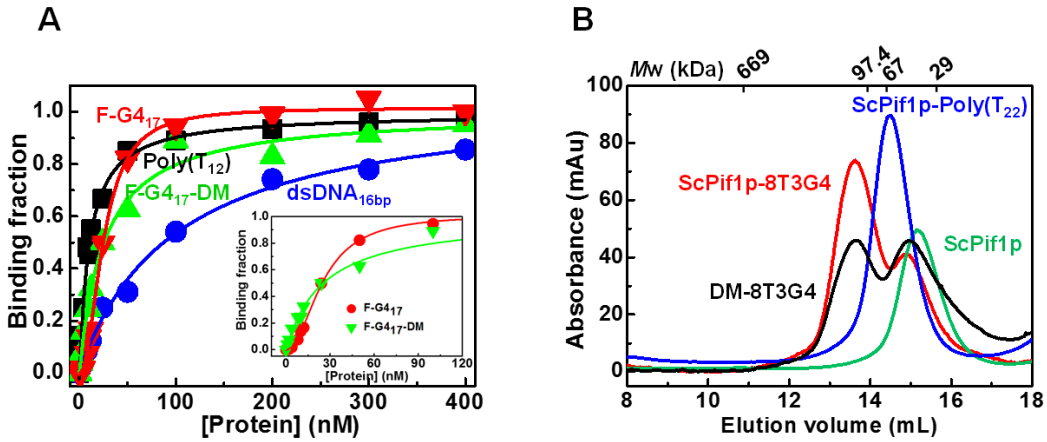
A
Binding fraction
[Protein] (nM)
F-G4$_{17}$
Poly(T$_{12}$)
F-G4$_{17}$-DM
dsDNA$_{16bp}$
B
Mw (kDa)
669
97.4
67
29
ScPif1p-Poly(T$_{22}$)
ScPif1p-8T3G4
ScPif1p
DM-8T3G4
Absorbance (mAu)
Elution volume (mL)

Table S1. DNA substrates used in various assays

Assay	Substrate	Sequence (5'–3')
Crystal	Poly(T_8)	TTTTTTTT
	Poly(G_3T_5)	GGGTTTTT
	Poly($T_3G_3T_2$)	TTTGGGTT
Unwinding	$S_{26}ds_{17}$	(dT_{26})ATGTATGTCAAGGAAGG-F[a] H[b]-CCTTCCTTGACATACAT
	$S_{26}G_4ds_{17}$	(dT_{26}) ($GGGTTA)_3$GGGATGTATGTCAAGGAAGG-F H-CCTTCCTTGACATACAT
Translocation	Poly(T_{54})	dT_{54}-Cy3
	Protein trap	dT_{56}
smFRET[c]	$smS_{26}G_4ds_{17}$	AAGCAGTGGTATCAACGCAGAGAAAT(iCy3) ($GGGTTA)_3$GGGATGTATGACAAGGAAGG Biotin-CCTTCCTTGTCAT(iCy5)ACAT
	$smS_{47}ds_{17}$	Cy3-(dT_{47})ATGTATGACAAGGAAGG Biotin-CCTTCCTTGTCAT(iCy5)ACAT
Binding	Poly(T_{12})	F-TTTTTTTTTTTT
	GR_{12}	F-GTGTGTGTGGTG
	F-RNA_{12}	F-CUCUGCUCGACG
	F-$G4_{17}$	F-AGGGTGGGTGGGTGGGT
	$dsDNA_{16bp}$	F-CTCTGCTCGACGGATT AATCCGTCGAGCAGAG
SAXS	GR_{11}	GTGTGGTGTGG
	8T11bp	TTTTTTTTCGCAGTGCTCG CGAGCACTGCG
	3G4	AGGGTTAGGGTTAGGGTTAGGG
	8T3G4	TTTTTTTTGGGTGGGTGGGTGGGT
DLS	Poly(T_{11})	TTTTTTTTTTT
	8T11bp	TTTTTTTTCGCAGTGCTCG CGAGCACTGCG
	8T3G4	TTTTTTTTGGGTGGGTGGGTGGGT

[a] F, fluorescein.
[b] H, hexachlorofluorescein.
[c] Single-molecule fluorescence resonance energy transfer.

Table S2. Data collection and refinement statistics

	ScPif1p SAD* **Poly(T_8)-ADP·AlF_4**	**ScPif1p-Poly(G_3T_5)-ADP·AlF_4**	**ScPif1p-Poly($T_3G_3T_2$)-ADP·AlF_4**	**ScPif1p-Poly(T_8)-ATPγS**
Data collection				
wavelength (Å)	0.9791	0.9791	0.9791	0.9778
Resolution range	44.15–3.16 (3.27–3.16)	58.71–2.03 (2.10–2.03)	65.21–3.34 (3.46–3.4)	65.0–3.28 (3.40–3.28)
Space group	P 21 21 21	P 21 21 21	P 31 2 1	P 21 21 21
Unit cell	74.2 90.9 185.6 90 90 90	75.2 88.3 187.7 90 90 90	150.6 150.6 136.3 90 90 120	74.4 90.8 186.2 90 90 90
Total reflections	254950 (25626)	506940 (21945)	274688 (22049)	116467 (12168)
Unique reflections	22200 (2148)	80210 (7015)	25042 (2024)	17964 (1952)
Multiplicity	11.5 (11.7)	6.3 (3.1)	11.0 (10.9)	6.5 (6.2)
Completeness (%)	99.6 (98.4)	98.1 (86.8)	95.4 (79.0)	89.7 (99.5)
Mean I/sigma (I)	13.43 (3.23)	17.01 (2.23)	17.23 (2.49)	7.62 (2.27)
Wilson B-factor	67.70	36.65	93.39	73.08
R-merge	0.14 (0.76)	0.06 (0.49)	0.17 (1.65)	0.16 (0.71)
CC1/2	0.99 (0.93)	0.99 (0.74)	0.99 (0.86)	0.99 (0.88)
Refinement				
Reflections used in refinement		80200 (7015)	24986 (2019)	17898 (1951)
Reflections used for R-free		3939 (355)	1253 (108)	950 (98)
R-work		0.19 (0.25)	0.17 (0.30)	0.25 (0.32)
R-free		0.23 (0.31)	0.25 (0.37)	0.32 (0.36)
Number of non-hydrogen atoms		9104	8456	8658
Protein residues		1035	1025	1054
RMS (bonds)		0.008	0.010	0.003
RMS (angles)		0.98	1.38	0.70
Ramachandran favored (%)		98.8	95.8	98.5
Ramachandran allowed (%)		1.2	4.2	1.5
Ramachandran outliers (%)		0.00	0.00	0.00
Rotamer outliers (%)		0.45	0.00	0.00
Clashscore		9.0	14.4	11.0
Average B-factor		54.4	114.7	82.9

***** Single wavelength anomalous dispersion.

Table S3. SAXS data collection and processing of DNA, ScPif1p and complexes

	3G4	**8T3G4**	**ScPif1p**	**ScPif1p-GR$_{11}$**	**ScPif1p-8T3G4 Peak 1**	**ScPif1p-8T3G4 Peak 2**	**ScPif1p-3G4 Peak 2**	**ScPif1p-8T11bp Peak 1**	**ScPif1p-8T11bp Peak 2**
Data-collection parameters									
Instrument	SWING	SWING	SWING	SWING	SWING	SWING	SWING	SWING	SWING
Beam geometry (mm)	0.4×0.1	0.4×0.1	0.4×0.1	0.4×0.1	0.4×0.1	0.4×0.1	0.4×0.1	0.4×0.1	0.4×0.1
Wavelength (Å)	1.03	1.03	1.03	1.03	1.03	1.03	1.03	1.03	1.03
q range (Å^{-1})	0.007-0.3	0.007-0.3	0.007-0.3	0.007-0.3	0.007-0.3	0.007-0.3	0.007-0.3	0.007-0.3	0.007-0.3
Data collection mode	HPLC	HPLC	HPLC	HPLC	HPLC	HPLC	HPLC	HPLC	HPLC
Exposure time (s) / nb frames	0.75 / 20	0.75 / 20	0.75 / 20	0.75 / 20	0.75 / 20	0.75 / 20	0.75 / 20	1 / 20	1 / 20
Concentration injected (mg.ml^{-1})	2	2	10	10	15	15	10	10	10
Temperature	288	288	288	288	288	288	288	288	288
Structural parameters									
I(0) (cm^{-1}) [from Guinier]	0.010	0.010	0.002	0.018	0.058	0.025	0.074	0.006	0.015
Rg (Å) [from Guinier]	12.3 ± 0.2	18.2 ± 0.2	29.3 ± 0.1	27.5 ± 0.3	42.8 ± 0.3	31.2 ± 0.3	42.9 ± 0.2	37.9 ± 0.1	29.0 ± 0.1
I(0) (cm^{-1}) [from $P(r)$]	0.010	0.010	0.002	0.018	0.058	0.024	0.074	0.006	0.015
Rg (Å) [from $P(r)$]	12.2	18.6	29.4	27.6	42.9	30.9	43.2	38.0	29.0
Dmax (Å)	40.5	63.0	100.7	90.8	149.5	103.3	150.0	124.9	93.6
Porod estimate (Å^3)	9662	18975	95642	97094	208344	105951	233153	198499	107489
Molecular-mass determination									
Partial specific volume (cm^3.g^{-1})	0.54	0.54	0.74	0.73	0.71	0.71	0.72	0.71	0.71
Contrast ($\Delta\rho \times 10^{10}$ cm^{-2})	6.28	6.28	2.82	2.95	3.27	3.27	3.16	3.25	3.25
Molecular mass M_r from I(0) (Da)	6039	10859	59776	61116	130215	66219	145720	124062	67180
Calculated monomeric M_r from sequence (Da)	6732	9216	61496	65034	70635	70635	68228	70441	70441
Data processing									
Primary data reduction	FOXTROT	FOXTROT	FOXTROT	FOXTROT	FOXTROT	FOXTROT	FOXTROT	FOXTROT	FOXTROT
Data processing	PRIMUS	PRIMUS	PRIMUS	PRIMUS	US-SOMO	US-SOMO	US-SOMO	US-SOMO	US-SOMO
Ab initio analysis	DAMMIF	DAMMIF	DAMMIF	MONSA	MONSA	MONSA	MONSA	MONSA	MONSA
Number of models	50	50	50	32	32	32	32	32	32
Model χ^2	1.44 ± 0.01	2.09 ± 0.01	4.24 ± 0.02	1.19 ± 0.01	4.13± 0.02	2.45 ± 0.02	1.28 ± 0.01	1.61 ± 0.01	2.22± 0.07
Validation and averaging	DAMAVER	DAMAVER	DAMAVER	DAMAVER	DAMAVER	DAMAVER	DAMAVER	DAMAVER	DAMAVER
NSD	0.55 ± 0.10	0.86 ± 0.20	0.92 ± 0.19	0.65 ± 0.12	0.84 ± 0.25	0.69 ± 0.10	0.66 ± 0.12	0.59 ± 0.10	0.65 ± 0.12
Rigid-body modeling	HYDROPRO	HYDROPRO	EOM	MODELLER	SASREF / EOM	SASREF / MODELLER	SASREF / EOM	SASREF / MODELLER	SASREF / MODELLER
Computation of model intensities	CRYSOL	CRYSOL	CRYSOL	CRYSOL	CRYSOL	CRYSOL	CRYSOL	CRYSOL	CRYSOL
Model χ^2	1.47	1.34	1.16	1.23	1.66	2.08	1.85	1.98	1.23

Table S4. Summary of physical parameters of SAXS assays

Sample	***R*g (Å)**	***D*max (Å)**	χ^2
apo ScPif1p			
Experimental	29.3	100.0	
Crystal structure model	27.5	84.2	9.83
EOM (flexible 2B + 2C)	29.4	101.2	1.16
ScPif1p-GR$_{11}$			
Experimental	27.5	89.3	
Crystal structure model	27.5	84.2	1.23
3G4			
Experimental	12.3	39.0	
PDB 3SC8	12.3	40.2	1.47
8T3G4			
Experimental	18.2	63	
model	18.4	64	1.34
ScPif1p-8T3G4 (monomer)			
Experimental	30.8	93.4	
model	29.6	93.2	2.08
ScPif1p-8T3G4 (dimer)			
Experimental	42.8	133.7	
Dimer 1 2:2	38.2	144.2	18.6
Dimer 2 2:2	Steric clashes of 3G4		
Dimer 2 2:1	42.7	137.2	1.66
Dimer 3 2:2	40.8	141.7	5.67
Dimer 4 2:2	45.3	147.2	4.97
ScPif1p-3G4 (dimer)			
Experimental	42.9	150.0	
Dimer 2 2:1	43.1	157.7	1.85
ScPif1p-8T11bp (monomer)			
Experimental	29.0	102.0	
model	28.6	109.2	1.23
ScPif1p-8T11bp (dimer)			
Experimental	37.6	118.4	
Dimer 2 2:1	37.2	111.2	1.98